SERS Biodetection Using Gold–Silica Nanoshells and Nitrocellulose Membranes

ARTICLE *in* ANALYTICAL CHEMISTRY · JUNE 2011

Impact Factor: 5.64 · DOI: 10.1021/ac103195e · Source: PubMed

7 AUTHORS, INCLUDING:

Sandra Whaley Bishnoi
Rice University
34 PUBLICATIONS **1,630** CITATIONS
SEE PROFILE

Vimal P Swarup
University of Utah
16 PUBLICATIONS **88** CITATIONS
SEE PROFILE

Timothy A Keiderling
University of Illinois at Chicago
276 PUBLICATIONS **7,394** CITATIONS
SEE PROFILE

analytical chemistry

ARTICLE

pubs.acs.org/ac

SERS Biodetection Using Gold–Silica Nanoshells and Nitrocellulose Membranes

Sandra Whaley Bishnoi,*[,†] Yu-jen Lin,[†] Martin Tibudan,[‡] Yiming Huang,[†] Marcelo Nakaema,[‡,§] Vimal Swarup,[†,⊥] and Timothy A. Keiderling*[,‡]

[†]Department of Chemistry, Illinois Institute of Technology, 3101 S. Dearborn Street, Chicago, Illinois 60616, United States

[‡]Department of Chemistry, University of Illinois, 845 West Taylor Street (m/c 111), Chicago, Illinois 60607-706 United States

Supporting Information

ABSTRACT: We have developed a rapid, reproducible, easy to execute, surface enhanced Raman scattering (SERS) method for detection of low volumes and total amounts of biological antigens using an analyte capture system derived from methods commonly used in Western blotting. Our method is a "half-sandwich" assay with an antigen detection scheme that employs a nitrocellulose (NC) membrane with 200 nm pore size to capture subnanograms of analyte and concentrate them in a small area from applied volumes as low as one microliter. The SERS probes used for detection consist of gold-silica nanoshells modified with a two-component mixed monolayer system. One component consists of a poly(ethylene glycol) (PEG)-modified Raman-active chromophore bound to the gold surface which allows for SERS detection and imparts particle stability. The second component uses (ortho-pyridyl) disulfide-PEG-succinimidyl ester to couple the recognition antibody to the particle surface. By controlling the reaction time and concentration of thiols, a mixed monolayer is prepared on the nanoshell surface with the ability to recognize low concentrations of analyte and generate reproducible SERS signals. Using this strategy, we have achieved SERS signals that are proportional to antigen present on the membrane allowing detection of total antigen amounts as low as 1.25 ng for some cases. The performance of this new SERS bioassay has been tested with a variety of potential antigens, demonstrating the potential for multiplexed detection of analytes.

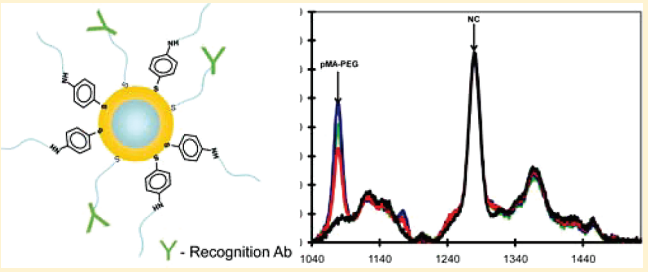

Over the last several decades many surface enhanced Raman scattering (SERS) methods have been developed for the detection of biological analytes with high specificity and sensitivity. Though these methods have improved dramatically, improvements are still needed in the areas of reproducibility, ease of use, and the ability to target specific analytes to move SERS from a niche detection method to a general analytical technique. High SERS enhancements have been achieved by use of aggregated metal nanoparticles, such as gold and silver colloids, that can produce local "hot spots" having SERS enhancements between 10^6 and 10^8 over normal Raman scattering signals for single molecules.[1,2] However, large fluctuations in SERS signals are often observed due to heterogeneity in cluster sizes and distribution of SERS "reporter" chromophores within the aggregates. One means to improve reproducibility of SERS signals has been the use of single nanoparticle plasmonic substrates, such as hollow gold nanospheres,[3] silver triangles,[4] gold nanorods,[5] and gold-silica nanoshells.[6] These materials have localized surface plasmon resonances (LSPRs) in the near-infrared part of the electromagnetic spectrum that couple well to the excitation lasers commonly used in Raman spectroscopy of biological species (633 and 785 nm), providing strong electromagnetic fields for SERS enhancement rather than relying upon the high junction potentials or "hot spots" that are properties of aggregates of small metal colloids[7] or necessitating additional particle growth steps, such as silver staining.[8,9] An additional benefit of using nanoshells is that their large scattering cross-section allows colorimetric detection at relatively low concentrations of particles.[10]

In addition to the choice in plasmonic enhancement vehicles, the design of SERS detection systems must also include (1) choice of the Raman chromophore, (2) method of chromophore attachment to the nanoparticle surface (or within the electromagnetic field of the particle), (3) incorporation of the antigen-recognition element, and (4) isolation of the antigen-SERS probe on some substrate to enable read out. The attachment of the Raman-active chromophore to the metal surface is often accomplished using (1) electrostatic attachment, which takes advantage of the electrostatic attraction between a negatively charged metal nanoparticle and positively charged Raman active chromophore,[11] (2) physisorption of the chromophore,[3] or 3) covalent attachment of the chromophores, generally using a thiol containing chromophore.[8]

Received: December 6, 2010
Accepted: April 19, 2011
Published: April 19, 2011

We have chosen to create a two component, self-assembled monolayer (SAM) system for SERS reporting and antigen detection. The first component provided SERS reporting and particle stability achieved using a PEG-modified chromophore, either p-mercaptoaniline (pMA) or 5-thio-2-nitrobenzoic acid (DNSB). These Raman chromophores were chosen because of their large Raman cross sections and ability to covalently bind to both the gold surface. Incorporation of PEG on the reporter group enhances particle stability in high ionic strength buffers.[12,13] The second component achieved antigen detection through incorporation of a recognition antibody to complete the SERS probe. This was prepared by combination of the selected antibody with a commercially available, bifunctional PEG (orthopyridyl disulfide-PEG-*n*-hydroxysuccinimide, OPSS-PEG-NHS) containing a thiol on one end of the PEG chain to bind to the nanoparticle surface and an NHS group on the other end to attach antibodies. This strategy allows direct covalent attachment of the selective component (antibody) to the surface of the nanoparticle, but avoids conformational constraint by placing it at the end of the PEG linker, and provides additional stabilization of the nanoparticles against aggregation in the buffered solutions needed.

Though significant effort has been put into the development of SERS probes for immunodetection of specific biomarkers, less attention has been paid to the substrates used for isolation of the antigen-SERS probe and allowing "off-line, asynchronous" readout of the assay. Many techniques rely on a solid support for the capture of biomarkers and utilize a sandwich assay methodology for selection and detection of the antigen. In many of these cases, the solid support (glass[14] or gold[15]) is first modified with a SAM, which is then modified with a capture antibody specific to the antigen.[16] This preparation often takes several hours prior to incubation with the antigen. The antigen is then allowed to incubate with the substrate for several hours prior to detection with the SERS probe. This process is tedious, requiring multiple blocking, washing, and incubation steps to prevent nonspecific attachment of other biological species. In addition, immobilization of a limited number of antigens relies upon diffusion limited processes and therefore long incubation times or large volumes of biological media are necessary for detection of antigen at low concentrations.[17] Nitrocellulose membranes (NCs) are known for their ability to bind proteins with strong affinity through hydrophobic−hydrophobic interactions and are used universally for extraction and stabilization of proteins in Western blotting assays.[18,19] In this study, we have expanded upon the use of NC for analyte capture to allow SERS detection by utilization of gold-silica nanoshells as SERS enhancement substrates and Raman active polyethylene glycols (PEGs) as detection chromophores. This facile immunoassay method can be further demonstrated to provide a means for multianalyte detection for small volumes (1 μL) of higher concentration antigen solutions, rather than the high volumes of low concentrations used under flow conditions. Such an antigen isolation technique simplifies assay construction and allows one to use extremely low volumes of antigen containing solutions, but still provides detection with high signal-to-noise (S/N) ratios and the specificity expected using traditional SERS immunoassay techniques. In addition, the Raman signal from the NC acts as an internal standard for normalization of spectra, increasing the reproducibility of the assay. An independent use of NC for analyte capture with SERS detection has also been recently reported.[9]

EXPERIMENTAL SECTION

Reagents. Para-mercaptoaniline (pMA), 1,3-dicyclohexylcarbodiimide (DCCD), *N*-hydroxysuccinimide (NHS), tetrahydrofuran (THF), acetonitrile, methoxypolyethylene glycol amine, dimethyl sulfoxide (DMSO), methoxypolyethylene glycol succinate N-hydroxysuccinimide (mPEG-NHS), phosphate buffer packs, and bovine serum albumin (BSA) were purchased from Sigma and used without further purification. Orthopyridyl disulfide-PEG-*n*-hydroxysuccinimide, OPSS-PEG-NHS, was purchased from JenKem Technology USA Inc. (Allen, TX). Nitrocellulose membranes (Protran 0.2 μm, 0.1 μm, and 0.4 μm pore) were obtained from Whatman (Dassel, Germany). Rabbit IgG (whole molecule no. 31235) was obtained from Thermo (Rockford, IL). Fluorescein (FITC)-conjugated AffiniPure Goat Anti-Rabbit IgG was obtained from Jackson ImmunoResearch Laboratories, Inc. (West Grove, PA). Affinity purified, HRP conjugated, bovine β-lactoglobulin (BLG) antibody was obtained from Bethyl Laboratories, Inc. (Montgomery, TX). Tris buffered saline (TBS) was obtained from Amresco (Solon, OH). Tween-20 was obtained from Bio-Rad (Hercules, CA). CNGB3, anti-CNGB3 antibody and bovine retinal lysate were gifts from Professor Deepak Edward's group at Summa Health System, Akron, Ohio, and used as received. The anti-CACNA1F antibody was a gift from Professor Brian Kay and Mr. Mike Kierny of the University of Illinois at Chicago.

Para-mercapto-aniline poly(ethylene glycol) 5000 (pMA-PEG) was synthesized according to recently published procedures[12] and stored at −20°C prior to use. Gold nanoparticles (60 nm diameter) were purchased from Ted Pella, Inc. Nanoshells were synthesized according to published procedures[20] and characterized using dynamic light scattering (Malvern Nano-S) and UV−vis spectrophotometry (V-530, Jasco) prior to use. The nanoshells were tuned so that the wavelength of maximum absorption (extinction) was near that of the excitation laser on the Raman spectrometer (785 nm).[6]

5,5′-dithiobis(succinimidyl-2-nitrobenzoate) (DSNB) was synthesized according to previously published procedures using a one-pot carbodiimide coupling of DCCD from a mixture of DNBA and NHS dissolved in THF.[21] The product was purified by recrystallization in acetone/hexane and purity tested using thin layer chromatography and stored at 4°C in the dark until needed. DSNB-PEG was synthesized by dissolving DSNB (3 mg, 0.006 mmol) in 1 mL acetonitrile and slowly adding it to 10 mg methoxypolyethylene glycol amine ($PEGNH_2$, 5000 MW, 10 mg, 0.002 mmol) in 50 μL of dimethyl sulfoxide (DMSO) and letting it react overnight. The resulting product was placed into a 3.5K MWCO dialysis cartridge (Slide-A-Lyzer, Pierce) and dialyzed against 100 mM, pH 8.0 phosphate buffer to remove excess DSNB, after which it was purified by extracting with dichloromethane and ultrapure water (18 MΩ, MQ). The product in the water portion was collected and lyophilized. The concentration of DSNB-PEG was obtained using a molecular extinction coefficient of 8123 $M^{-1}cm^{-1}$ at 350 nm, obtained from measuring known concentrations of DNBA (the chromophore in DSNB) in THF.

Antibody Conjugate Synthesis. First, orthopyridyl disulfide-PEG-n-hydroxysuccinimide (OPSS-PEG-NHS) was dissolved in potassium carbonate buffer (100 mM, pH 9.3) to achieve a final concentration of 1.5 mg/mL. Ten μL of this solution was immediately added to 490 μL of recognition antibody dissolved in potassium carbonate buffer (450 μg total antibody). The solution was gently mixed and then allowed to react overnight on ice.

Raman Probe Synthesis. The nanoshell (NS) probes were synthesized by addition of 6 μL of antibody conjugate (0.9 mg/mL) to 1 mL of nanoshell solution ($\lambda_{max} \approx 780$ nm, Abs =1.5) and incubated overnight on ice to allow sufficient antibody coverage on the nanoshell surface. To this solution, 30 μL of Raman-active PEG (either pMA-PEG or DSNB-PEG) at a concentration of 1×10^{-4} M was added to obtain a final Raman chromophore concentration of 3×10^{-6} M. This solution was incubated for 25 min on ice prior to purification by centrifugation at 3000 rpm (Eppendorf Mini-Spin) for 6 min and then the pellet was resuspended in MQ water.

Raman Immunoassay. Antigen spots (2.5 mm diameter was used here, although other sizes were tested) were created on NC by depositing 2 μL of diluted antigen onto a NC membrane section placed on a stack of filter paper to wick solvent away. This was dried on the bench for 15 min, effecting a concentration and stabilization of the antigen on the NC, after which the NC membrane was immersed in blocking buffer (5% BSA in TBS with 1% Tween-20, TBST) and agitated for 45 min. Membranes were then removed and immediately placed in a solution containing the NS probe (3×10^9 NS/mL) and rocked for 35 min to prevent probe sedimentation, after which they were washed in a soft stream of MQ water to remove excess probe. Membranes were then immersed in cold TBST and agitated on an orbital shaker for 15 min to remove nonspecifically bound nanoshell probe. The washing process was repeated as necessary. Membranes were stored at 4 °C until spectral analysis.

For detection of multiple antigens on the same NC membrane, two methods were tested: (1) simultaneous exposure of the NC membrane by mixing equal quantities of the NS probes for each antigen and (2) serial exposure of NC membrane to one NS probe followed by rinsing with cold TBST and then subsequent exposure to the second NS probe.

Raman Spectroscopy/Microscopy. Two Raman systems were used for determination of binding between the NS probe and antigen on the NC surface. The first system was a Renishaw Raman microscope (in Via, Renishaw, Gloucestershire, UK). Spectra were typically collected in a backscattered geometry through a 5× (NA = 0.08) microscope objective, although higher magnifications were tested. The excitation source was a 785 nm diode laser (8 mW laser power available at sample) with a spot size of ~15 μm. The spectrometer was routinely calibrated with a silicon wafer. Data points used for the final analyses resulted from averaging five spectral accumulations of 60 s acquisition time at each step and summing measurements taken for six steps collected across the antigen spot, where steps are ~100 μm apart.

Raman measurements were also performed with a micro-Raman instrument constructed at UIC based on a modified Nachet microscope for sampling the NC surface in a back-scattering geometry and transferring the scattered light to a spectrograph and CCD. This setup had multiple lasers and the possibility of shifting spectral ranges and obtaining fluorescence from chromophore-labeled antibody samples. For the SERS data reported herein, illumination used a 785 nm diode laser (Innovative Photonic Solutions) which was filtered (MaxDiode, Semrock) to avoid unwanted wavelengths and then reflected to the back aperture of a 10X microscope objective lens (Olympus, NA 0.25) by a 45° dichroic mirror (RazorEdge, Semrock). The beam spot size on the NC surface was experimentally determined to be 50 μm, or a bit less, and the laser power there was ~26 mW. The larger spot size effectively averaged data from many deposited nanoparticle probes, thereby reducing fluctuation in signal. The scattered light was recollected by the same objective lens and focused on the monochromator entrance slit by an f/4 lens. Its nonelastic component was transmitted (>95%) through the same dichroic mirror used for excitation which in this direction blocked most of the laser line, and any remaining elastic component was blocked by a long pass filter (RazorEdge, Semrock). Detection of the Raman spectrum used a Jobin-Yvon HR640 monochromator with a 600 g/mm grating and a back-thinned, deep-depleted CCD detector (Newton 920N-BRDD, Andor Technology). The CCD detector output was calibrated by using known Raman transitions of crystalline silicon and cyclohexane whose positions were fit to a second-order polynomial equation in order to obtain the wavenumber conversion factor. A secondary calibration used the Raman transitions of the NC as an internal correction.

Scanning Electron Microscopy. Two deposits of 20 ng IgG and two controls were created on NC membranes, blocked with BSA, and then exposed to anti-IgG/pMA-PEG NS probe. After rinsing with TBST, the deposited sample areas were cut out of the NC and mounted onto aluminum specimen holders for scanning electron microscopy (SEM) analysis. One IgG sample and one control were coated with 8 nm of palladium−platinum prior to imaging on a high resolution JEOL JSM-6320F field emission scanning electron microscope at 20 000× magnification with a 6 kV accelerating voltage and 9.0 mm working distance. The other two samples, IgG and control, were imaged using a Hitachi S-3000N Variable Pressure-SEM with a chamber pressure of 20 Pa with a 20 kV accelerating voltage and 15.0 mm working distance. The Hitachi S-3000N was equipped with an energy dispersive X-ray spectrometer, Inca EDX system (Oxford) with a light element X-ray detector, and was used to identify elements present.

RESULTS AND DISCUSSION

Gold−silica nanoshells were designed to have a maximum absorption, corresponding to their plasmon resonance, at ~780 nm using published methods.[20] Using these nanoshells, SERS probes were constructed using a mixed monolayer system consisting of Raman-active PEGs[13] and OPSS-PEG-antibody conjugates[22] (schematically illustrated in Figure 1 A and B, upper panel). The SERS activity of each synthesized probe was confirmed by spotting 10 μL of the probe solution (3×10^9 NS/mL) onto a quartz slide and measuring the Raman intensity at either 1078 cm^{-1}, corresponding to the ring breathing mode of pMA-PEG,[13] or 1340 cm^{-1} corresponding to the symmetric stretching of NO_2 in DSNB-PEG.[21] To determine whether the recognition antibody of the probe was simultaneously bound to the NS surface, we initially deposited 100 ng (2 μL of 50 ng/μL) of the corresponding antigen onto a NC membrane segment and exposed the NC to a solution of the NS probe conjugated with the PEG-antibody and SERS reporter functionalities. This provided a positive control as well as a test of the probe's ability to selectively bind to the sample area. Due to the large scattering cross-section of nanoshells,[10] a blue-green spot could be seen on the membrane at high antigen concentration if the probe successfully bound the antigen after excess probe was removed with multiple rinsing. A parallel test was done by construction of probes using colloidal gold nanoparticles of 60 nm diameter but gave less signal, and that approach was not tested further.

An initial test of our half-sandwich assay was done using rabbit IgG as the antigen. When 5 ng of rabbit IgG was spotted onto NC, exposed to the anti-IgG Raman-active probe, and analyzed,

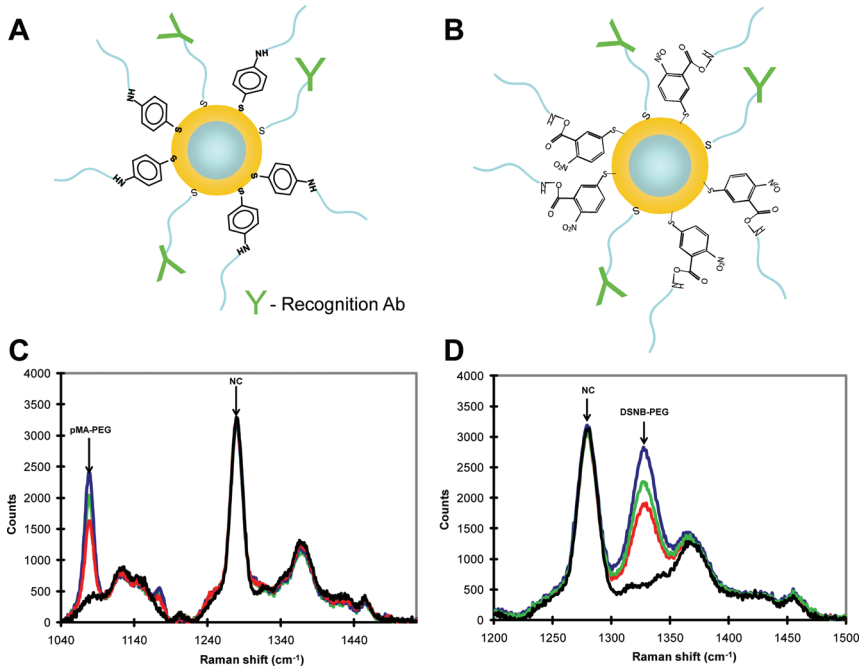

Figure 1. (A and B) Schematic representations of (A) pMA-PEG/anti-IgG and (B) DSNB-PEG/anti-IgG NS probes. (C and D) Raman spectra collected from NC membranes (blue, red, and green) with three sample depositions with 5 ng of IgG and a control (blank) deposition (black) after exposure to either (C) pMA-PEG/anti-IgG or (D) DSNB-PEG/anti-IgG NS probes. The spectra demonstrate that the probes bind different antigens well, yield large SERS signals and have sample-to-sample variation in the probe Raman signal at 1078 (C) and 1340 cm^{-1} (D), but show relatively little nonselective background binding of probe. The Raman signal emanating from the NC membrane (1288 cm^{-1}) is used as an internal standard, which is the source of its consistency here. Spectra were collected using the UIC micro-Raman instrument. Each spectrum represents the average of six steps taken across antigen deposition as described in the Experimental Section.

the signal clearly indicated probe recognition of the IgG antigen (Figure 1C and D). The NC peaks provide a consistent background signal, seen in the scans of the negative control obtained by depositing just the buffer, no antigen (black traces), that are composed of a broad background and a few intense features (e.g., 1288 cm^{-1}) that do not significantly interfere with the Raman signals of the pMA-PEG (Figure 1A, 1078 cm^{-1}) or DSNB-PEG (Figure 1B, 1340 cm^{-1}). The control shows no noticeable spectral response in that the area under the characteristic pMA or DSNB peaks indicating that nonspecific binding is not a significant problem. Spectra taken from multiple points within the antigen spot varied in intensity with the laser focus position used but the spectra were essentially the same for each scan giving the analysis qualitative consistency for either of the two SERS probes (Figure 1C and D). Because of the heterogeneity of the antigen deposition within a sample, six points obtained on a scan within the sample area were summed to yield the individual spectra in Figure 1. These values still show variations for separate sample depositions, suggesting the need to average data over several samples. A demonstration of the positional dependence of the signal as the laser is scanned across the spot is provided in Figure S1, Supporting Information, showing reproducible variations for different Raman bands which indicates that the dependence originates in the heterogeneous particle (probe) density and is not because of noise or detection limit. An alternate point of view is provided by imaging the sample via its Raman intensity, which shows random probe deposition, see Supporting Information, Figures S2 and S3.

To better understand this probe deposition heterogeneity, two samples containing 20 ng of Rabbit IgG and two controls were created on NC and then taken through the steps of our half-sandwich immunoassay, as described above. One antigen containing spot and one control spot were cut out of the membrane, coated with a thin layer of PtPd, and imaged using a JEOL field emission scanning electron microscope (Figure 2A and C, respectively). The other two spots (antigen and control) were imaged without coating using a Hitachi variable pressure scanning electron microscope (Figures 2B and D, respectively). The high-resolution SEM results (Figure 2A) give a good indication of the irregular spatial distribution of the NS probe particles on the NC membrane for these small sample deposits, as well as illustrate details regarding the structure of the membrane. However, in the control (blank) spot, no NS probe particles were detected (Figure 2C), as is consistent with the SERS results discussed above and shown in Figure 1 C and D, spectra of the controls (black traces). From the lower resolution SEM micrographs of the NC without PtPd coating, it was clear that the antigen containing spot (Figure 2B) had a significantly greater amount of high electron density containing material, assumed to be the gold NS, while the control spot did not contain such material (Figure 2D). Moreover, energy dispersive X-ray spectra from the high electron-density spots gave further strong evidence indicating the presence of NS probe particles. Two significant features were detected at 2.12 and 9.71 keV, corresponding to the characteristic X-ray L and Kα lines for gold (Figure 2E). The presence of the silicon peak at 1.74 keV helped confirm that the high electron density seen by SEM in Figure 2B came from the Au-silica nanoshells used to make the probe particles.

Once it was determined that the SERS probes were capable of detecting the presence of antigen on the NC surface (Figures 1 and 2),

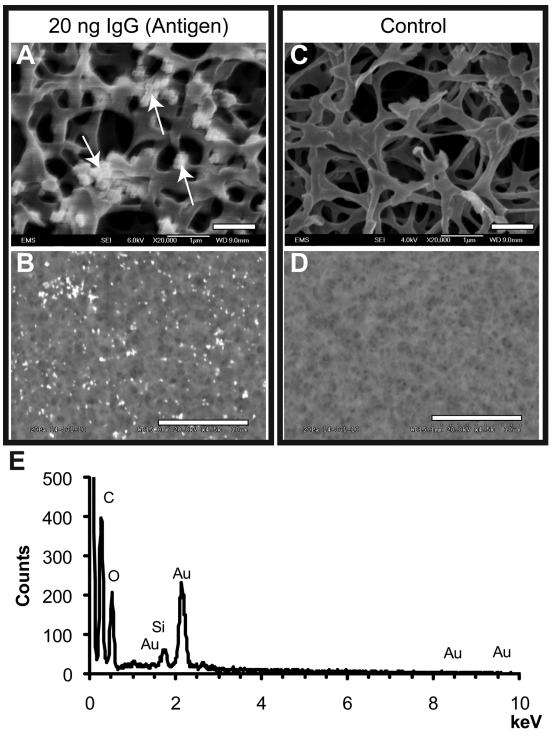

Figure 2. (A and C) High resolution scanning electron microscopy results from NC containing (A) 20 ng IgG (antigen) and (C) a control spot without antigen, both exposed to NS probe (JEOL JSM-6320F FE-SEM 20,000X Magnification, 6 kV Accelerating voltage, 9.0 mm WD, coated with PtPd). (B and D) Variable pressure scanning electron microscopy results for uncoated NC membranes containing (B) antigen and probe or (D) control spot and probe (Hitachi S-3000N Variable Pressure-SEM, Pressure = 20 Pa, 20 kV Accelerating voltage, 15.0 mm WD). (E) Energy dispersive X-ray spectrum of a NS particle found in (B) (Oxford Inca EDX system with a light element X-ray detector, 15 mm WD). The white bars on the EM images indicate the length scale, 1 μm for A and C and 10 μm for B and D.

the Raman probe detection sensitivity for antigen immobilized on a NC membrane was tested using serial dilutions of a model antigen (IgG). Antigen amounts ranging from 20 ng (2 μL of 10 μg/mL) to 0.8 ng (2 μL of 0.4 μg/mL), were placed onto NC and exposed to either the anti-IgG/pMA-PEG NS probe (Figure 3A) or the anti-IgG/DSNB-PEG NS probe (Figure 3C). Each NC section contained four test sample deposition areas, with three having the same amount of IgG and one blank with only PBS deposited as a negative control. Each spectrum in Figure 3A and 3B represents the average over three test spots (to get an impression of the spot-to-spot variation, the spectra that were averaged over the six steps in each spot corresponding to Figure 3A are given in the Supporting Material, Figure S5). Normalization of the peaks by dividing by the intensity of the NC membrane signal at 1288 cm^{-1} provides a correction for variations in Raman efficacy due to local irregularities in the scattering from the sample or laser exposure.

As shown in Figure 3, the anti-IgG/pMA-PEG NS probe (Figure 3A) and the anti-IgG/DSNB-PEG NS (Figure 3C) exhibit strong Raman peaks for spots containing 20 ng of rabbit IgG. The normalized intensity of the DSNB-PEG peak (1340 cm^{-1}) is much higher (scale change of 5) than the pMA-PEG peak (1078 cm^{-1}), which is most likely due to the large Raman scattering cross section from the nitro group of DSNB-PEG.[23] As the concentration of IgG antigen decreased, Raman signals from IgG/pMA-PEG probes (Figure 3b) gradually declined to a low level for which a clear, but weak feature is evident in the spectra at 1.25 ng and a response that can be differentiated from the control can be seen in the spectra for the 0.8 ng sample. By comparison, signals of IgG/DSNB-PEG (Figure 3d) declined more dramatically providing a detectable signal still at 2.5 ng. If one were to define a detection limit based on the standard deviation of these data (3σ), it would be higher than these values due to the sample to sample variation, not to noise or fundamental detection ability of the spectra. As the sample antigen amounts are decreased, the SERS bands remain identifiable but have large amplitude variations, so that the standard deviations are large. More extensive averaging over the sample deposition, including 2-D scans, can improve the statistics, lower the standard deviation and consequently enhance the detection limit. This is demonstrated qualitatively in the Supporting Information, Figure S4, where data gathered under different conditions is averaged for 50 samples across an image, and the standard deviations are improved. These actually should be worse, since a smaller laser spot was used, but the averaging addresses the main source of error, sample inhomogeneity and consequent sparseness of probe in the sample area when measuring small amounts of antigen. Dose response curves, following the style of Wang, et al.[15] taken from the data for the two probe systems in Figure 3A and C are shown below the corresponding spectra as Figure 3B and D, respectively.

One possible reason for the differences in the sensitivity of the two probes may be due to variations in the stability of these probes during the washing or incubation processes of the assay. Previous results showed that the pMA-PEG stabilized NS against aggregation better than commercially available PEG-SH, which is most likely due to the *para*-mercaptoaniline ring's ability to π-stack, allowing it to improve the self-assembled monolayer formed on the NS surface.[12] However, in the case of the DSNB-PEG used in this work, the PEG chains are in the *meta*-position of the aromatic ring instead of the *para*-position, which may sterically hinder π-stacking of rings and thereby reduce the stability of the DSNB-PEG probes.

Following the initial testing using the IgG antigen, we modified our method to detect a smaller protein antigen, bovine beta-lactoglobulin. BLG (MW 18.2 kDa), a globular protein found in the whey protein of cow's milk, provided an alternative target, unrelated to IgG, for determining whether this technique was capable of detecting a wider variety of protein antigens. In our system, 2 μL of BLG was spotted onto the NC membrane at 200 ng and 20 ng, and then detected using a mixed-monolayer consisting of OPSS-PEG linked rabbit anti-BLG and pMA-PEG on the NS surface. To determine the specificity of the anti-BLG/pMA-PEG probes, four other proteins (goat antirat IgG, mouse antihuman vWF, mouse anti-Rho, and rat antimouse integrin) and PBS were spotted as controls and exposed to the anti-BLG/pMA-PEG NS probes. Raman measurements were done under the same conditions outlined above at six different locations in each spot. The peak intensities of anti-BLG/pMA-PEG NS probes (1078 cm^{-1} from pMA-PEG) were normalized using the NC membrane peak at 1288 cm^{-1}, after background subtraction. On the membrane, spots containing 200 ng and 20 ng BLG were obvious from the blue-green stain present because of NS absorption, and strong Raman intensities were obtained, indicating the capability of the NS SERS probe to detect a small protein antigen. Three of the control spots, Mouse antihuman vWF, Mouse anti-Rho, and PBS, had little to no detectable

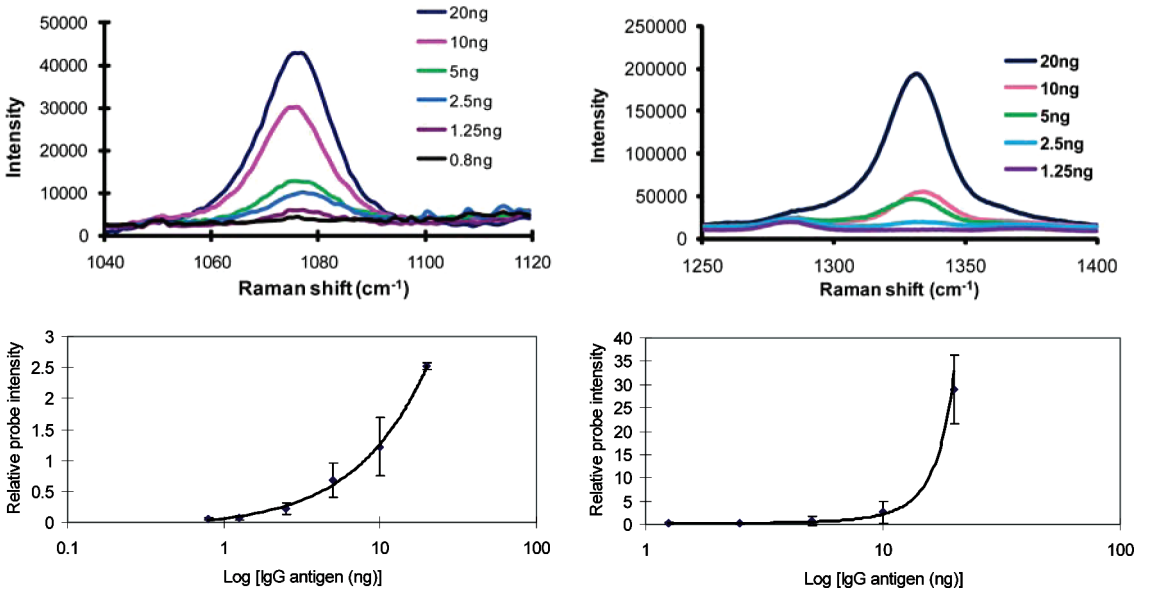

Figure 3. SERS response of Raman NS probes using a model antigen (IgG). Raman spectra (A) of anti-IgG/pMA-PEG NS probe as a function of antigen amount and (C) of anti-IgG/DSNB-PEG NS probe as a function of antigen (IgG) amount. Each probe demonstrated a SERS response that was proportional to the antigen concentration. Corresponding dose−response curves are shown in B and D respectively. Intensities are shown after background subtraction and normalization with the NC membrane peak at 1288 cm^{-1}.

Figure 4. Bovine β-lactoglobulin (BLG) was deposited onto NC at 200 ng and 20 ng total protein. The detection of the protein was accomplished using a rabbit anti-BLG/pMA-PEG NS probe and compared to the detection of 20 ng of control proteins (goat anti-Rat IgG, mouse antihuman vWF, mouse antirhodopsin, rat antimouse integrin) and PBS. Intensities shown are after background subtraction and normalization with the NC membrane peak at 1288 cm^{-1}.

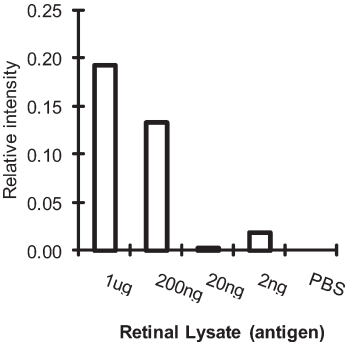

Figure 5. Phage display-derived, Anti-CACNA1F expressed antibody-based probe was used to detect the presence of the membrane-bound protein, CACNA1F, in the presence of serial dilutions of a bovine retinal lysate. Intensities are shown after background subtraction and normalization with the NC membrane peak at 1288 cm^{-1}.

Raman signal, consistent with the lack of affinity to the anti-BLG detection antibody; however the Goat antirat IgG and the Rat antimouse integrin spots indicated some weak nonspecific binding of the BLG probe. This nonspecific binding was present in repeated experiments, implying the cross-reactivity of the antibodies. Even considering the existence of cross-reactivity, the response of the NS probes to BLG antigens at 20 ng was significantly more intense than to the controls at the same concentration. These results demonstrate that our SERS detection method can discriminate among antigens and thus has promise for multiplex testing of various antigens captured on a NC membrane by modifying the detection antibody bound to the NS probe surface.

In bioassays, antigen detection from whole lysate sample using biosensors is the desired approach for clinical diagnostics; since separation and purification of an antigen from the lysate is always time-consuming. To test the efficiency of our method in such conditions, bovine retinal lysate was acquired from Prof. Deepak Edward (Northeastern Ohio University). Two-component NS probes were created using self-assembly of pMA-PEG and OPSS-PEG-anti-CACNA1F. The anti-CACNA1F antibody was provided by Prof. Brian Kay and Mike Kierny, UIC, after it was isolated using a phage display system and then expressed as a Fab-fragment in *E. coli*. This antibody was developed to recognize a peptide sequence corresponding to a membrane-bound protein, CACNA1F (also known as $Ca_v1.4$), present in retinal lysate. The lysate sample was serially diluted, and 2 μL was spotted onto the NC membrane for total protein deposition ranging from 1 μg to 2 ng. These were exposed to the anti-CACNA1F/pMA-PEG NS probes using the same protocol described above. Figure 5 summarizes the detection results after the pMA-PEG intensities at 1078 cm^{-1} were normalized using the NC membrane peak at 1288 cm^{-1}. In this bar chart, a reliable response was obtained when the amount of retinal lysate present was above 200 ng. Though

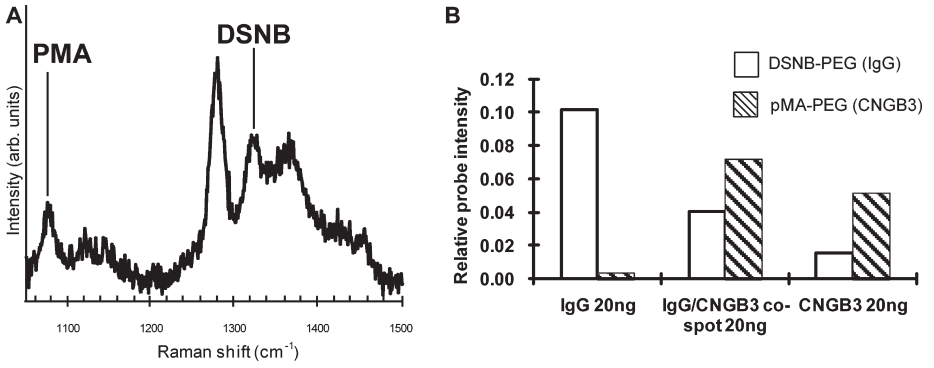

Figure 6. (A) SERS spectra of the simultaneous detection of 20 ng of IgG (DSNB-PEG probe) and 20 ng of a cyclic nucleotide gated channel beta 3 peptide (CNGB3, pMA-PEG probe). (B) Bar chart showing relative signals of sample depositions containing individual antigen and comixed antigens after background subtraction and normalization with the NC membrane peak at 1288 cm^{-1}.

this might appear to be a much lower sensitivity than found with the previous pure antigen systems, it is actually still quite good, since the amount of antigen present was significantly lower than the total amount of unpurified lysate spotted (probably <1%).[24] More interestingly, these results provided proof that our technique could be used for selective analysis in complex unpurified biological solutions by using designed antibodies to construct probes with specific target antigen affinity. In addition, the design of this test and its success demonstrates that the recognition element immobilized onto the NS surface does not have to be a full IgG antibody and that smaller recognition units, such as Fab fragments, are sufficient for antigen detection with our method.

The above results demonstrated high sensitivity Raman detection of three different types of antigen and showed good potential for design of a simultaneous multiplexed assay. Figure 6 demonstrates functionality of such a prototype multiplexed assay to simultaneously detect two antigens, a cyclic nucleotide gated channel beta 3 protein (CNGB3) and IgG. The CNGB3-specific probes were tagged with pMA-PEG and the IgG-specific probes were tagged with DSNB-PEG, to provide discrimination in the SERS analysis. Four samples, 20 ng of CNGB3, 20 ng of IgG, 20 ng of mixed-CNGB3 and IgG, and PBS (blank) were deposited onto NC, which was then incubated in a mixture of two probes (CNGB3/pMA-PEG and IgG/DSNB-PEG). Figure 6a shows the SERS spectrum of the mixed antigen spot that has a 1078 cm^{-1} peak from anti-CNGB3/pMA-PEG NS probes and 1340 cm^{-1} peak from anti-IgG/DSNB-PEG NS probes, indicating both probes can bind and separately detect to the two antigens in this spot. In the bar chart representing the averages over the spots (Figure 6b), the IgG antigen spot showed a high intensity response for the anti-IgG/DSNB-PEG NS probe and had very little background binding for the anti-CNGB3/pMA-PEG NS probe. For the CNGB3 antigen spot, the signal from the anti-CNGB3/pMA-PEG NS probe was also was quite strong; however, there was a significant amount of background binding of the DSNB probe. This may be due to the fact that this probe was less stable in saline solutions, which increased its background binding. Finally, the bar graph representation (Figure 6b) of the spectrum in Figure 6a for the spot that contained both antigens (IgG and CNGB3) showed discriminating responses for both of the NS probes, demonstrating successful multiplexed detection. However, it would be expected that the DSNB probe should provide a relatively higher signal in the mixed antigen spot than was observed, since it has a significantly higher Raman cross-section. Thus, at this point we must consider the method to be a qualitative multiplexed assay, which can indicate the presence of multiple antigens but is not yet capable of the kind of sensitivity seen for one antigen alone. This simplified multiplexed assay can straightforwardly be expanded to a larger variety of antigens by changing the reporter molecules present on the NS probe surface.

CONCLUSIONS

In conclusion, we have developed a SERS-based bioassay that allows for simple sample preparation and requires only very low sampling volumes containing the target antigens. Nitrocellulose membranes were used as an antigen capture and concentration platform for the half sandwich assay, and the Raman peak arising from the membrane was used as an internal standard. PEG-modified chromophores were chosen to provide particle stabilization in biological media and to yield significant Raman signal as SERS reporters. Recognition antibodies were covalently conjugated to the nanoshell surface using a commercially available linker (OPSS-PEG-NHS), allowing facile preparations from off-the-shelf components for SERS detection. This technique has the ability to detect a large variety of antigens from large IgGs (MW 160 kDa) to smaller globular proteins, such as CNGB3 and BLG with relatively high specificity. In addition, both full IgG recognition antibodies and expressed Fab subunits have been shown capable of antigen recognition after immobilization on the nanoshell surface. Using a second Raman-active PEG, DSNB-PEG, qualitative detection of two antigens present on the same nitrocellulose membrane was achievable. This mixed self-assembled recognition and reporting layer technique can be easily applied to other nanosystems, such as colloidal gold and nanorods. As a test, we also used commercial nanoshells (AuroShell particles) provided by Nanospectra Biosciences (Houston, Texas) as SERS enhancers in this study, and similar results were obtained. By modifying the composition of the mixed-monolayer, this assay shows a good potential for use in a variety of clinical detections. Overall, this technique allows for the straightforward creation of SERS biodetection assays.

ASSOCIATED CONTENT

Supporting Information. Detailed plots of the variations in Raman intensities across and between sample spots and 2-D Raman images of the sample deposition distribution and analyses

of their variability are provided. This material is available free of charge via the Internet at http://pubs.acs.org.

AUTHOR INFORMATION

Corresponding Author

*E-mail: bishnoi@iit.edu (S.W.B.); tak@uic.edu (T.A.K.). Fax: 312-567-3494 (S.W.B.); 312-996-0431 (T.A.K.).

Present Addresses

[§]Department of Physics, Universidade de Alfenas, Alfenas, Brazil. [⊥]Department of Bioengineering, University of Utah, Salt Lake City, UT.

ACKNOWLEDGMENT

This work was supported by a grant from the Office of the Air Force Surgeon General (Contract number FA7014-07-C-0047) for which we are grateful. We thank Professor Deepak Edward (Northeastern Ohio University, College of Medicine, Akron) for supplying us with lysate samples and antibodies and Professor Brian Kay and Mr. Mike Kierny for providing us with expressed antibody and peptides. Anjan Roy assisted with some of the instrument development and subsequent data checking.

REFERENCES

(1) Moskovits, M. *Rev. Mod. Phys.* **1985**, *57*, 783–826.
(2) Baker, G. A.; Moore, D. S. *Anal. Bioanal. Chem.* **2005**, *382*, 1751–1770.
(3) Chon, H.; Lee, S.; Son, S. W.; Oh, C. H.; Choo, J. *Anal. Chem.* **2009**, *81*, 3029–3034.
(4) Camden, J. P.; Dieringer, J. A.; Zhao, J.; Van Duyne, R. P. *Acc. Chem. Res.* **2008**, *41*, 1653–1661.
(5) Temur, E.; Boyacı, İ.; Tamer, U.; Unsal, H.; Aydogan, N. *Anal. Bioanal. Chem.* **2010**, *397*, 1595–1604.
(6) Jackson, J. B.; Westcott, S. L.; Hirsch, L. R.; West, J. L.; Halas, N. J. *Appl. Phys. Lett.* **2003**, *82*, 257–259.
(7) Haynes, C. L.; Duyne, R. P. V. *J. Phys. Chem. B* **2003**, *107*, 7426–7433.
(8) Cao, Y. C.; Jin, R.; Mirkin, C. A. *Science* **2002**, *297*, 1536–1540.
(9) Manimaran, M.; Jana, N. R. *J. Raman Spectrosc.* **2007**, *38*, 1326–1331.
(10) Lin, A. W. H.; Lewinski, N. A.; Lee, M.-H.; Drezek., R. A. *J. Nanopart. Res.* **2006**, *8*, 681–692.
(11) Qian, X.; Peng, X. H.; Ansari, D. O.; Yin-Goen, Q.; Chen, G. Z.; Shin, D. M.; Yang, L.; Young, A. N.; Wang, M. D.; Nie, S. *Nat. Biotechnol.* **2008**, *26*, 83–90.
(12) Huang, Y.; Swarup, V. P.; Bishnoi, S. W. *Nano Lett.* **2009**, *9*, 2914–2920.
(13) Levin, C. S.; Bishnoi, S. W.; Grady, N. K.; Halas, N. J. *Anal. Chem.* **2006**, *78*, 3277–3281.
(14) Song, C. Y.; Wang, Z. Y.; Zhang, R. H.; Yang, J.; Tan, X. B.; Cui, Y. P. *Biosens. Bioelectron.* **2009**, *25*, 826–831.
(15) Wang, G.; Park, H.-Y.; Lipert, R. J.; Porter, M. D. *Anal. Chem.* **2009**, *81*, 9643–9650.
(16) Porter, M. D.; Lipert, R. J.; Siperko, L. M.; Wang, G.; Narayanana, R. *Chem. Soc. Rev.* **2008**, *37*, 1001–1011.
(17) Wang, G. F.; Driskell, J. D.; Porter, M. D.; Lipert, R. J. *Anal. Chem.* **2009**, *81*, 6175–6185.
(18) Towbin, H.; Staehelin, T.; Gordon, J. *Proc. Natl. Acad. Sci. U.S. A.* **1979**, *76*, 4350–4354.
(19) Han, X. X.; Jia, H. Y.; Wang, Y. F.; Lu, Z. C.; Wang, C. X.; Xu, W. Q.; Zhao, B.; Ozaki, Y. *Anal. Chem.* **2008**, *80*, 2799–2804.
(20) Oldenburg, S. J.; Averitt, R. D.; Westcott, S. L.; Halas, N. J. *Chem. Phys. Lett.* **1998**, *288*, 243–247.
(21) Grubisha, D. S.; Lipert, R. J.; Park, H.-Y.; Driskell, J.; Porter, M. D. *Anal. Chem.* **2003**, *75*, 5936–5943.
(22) Hirsch, L. R.; Jackson, J. B.; Lee, A.; Halas, N. J.; West, J. *Anal. Chem.* **2003**, *75*, 2377–2381.
(23) Driskell, J. D.; Kwarta, K. M.; Lipert, R. J.; Porter, M. D.; Neill, J. D.; Ridpath, J. F. *Anal. Chem.* **2005**, *77*, 6147–6154.
(24) Sinnegger-Brauns, M. J.; Huber, I. G.; Koschak, A.; Wild, C.; Obermair, G. J.; Einzinger, U.; Hoda, J.-C.; Sartori, S. B.; Striessnig, J. *Mol. Pharmacol.* **2009**, *75*, 407–414.